

Adaptive damage retention mechanism enables healthier yeast population

Qasim Ali^{1,2}, Riccardo Dainese^{1,3}, Marija Cvijovic^{1*}

¹Department of Mathematical Sciences, Chalmers University of Technology and University of Gothenburg, Gothenburg, Sweden

² Department of Mathematics, North Carolina State University, NC 27607, USA (current affiliation)

³ Laboratory of Systems Biology and Genetics, Institute of Bioengineering, School of Life Sciences, École Polytechnique Fédérale de Lausanne (EPFL), Lausanne, Switzerland (current affiliation)

*Corresponding author

Marija Cvijovic

Department of Mathematical Sciences

Chalmers University of Technology and University of Gothenburg

Chalmers tvärgata 3

SE-41296 Gothenburg, Sweden

Phone: +46 31 772 53 21

Email: marija.cvijovic@gu.se

22

23

Abstract

24 During cytokinesis in budding yeast, *Saccharomyces cerevisiae*, damaged proteins are
25 distributed asymmetrically between the daughter and the mother cell. Retention of damaged
26 proteins is a crucial mechanism ensuring a healthy daughter cell with full replicative potential
27 and an ageing mother cell. However, the protein quality control (PQC) system is tuned for
28 optimal reproduction success that suggests optimal health and size of the population, rather
29 than long-term survival of the mother cell. Modelling retention of damage as an adaptable
30 mechanism, we propose two damage retention strategies to find an optimal way of decreasing
31 damage retention efficiency in order to maximize population size and minimize the damage
32 in the individual yeast cell. A pedigree model is used to investigate the impact of small
33 variations in the strategies over the whole population. These impacts are based on the
34 altruistic effects of damage retention mechanism and are measured by cost function whose
35 minimum value provides the optimal health and size of the population. We showed that
36 fluctuations in the cost function allow yeast cell to continuously vary its strategy, suggesting
37 that optimal reproduction success is a local minimum of cost function. Our results suggest that
38 a rapid decrease in the efficiency of damage retention, at the time when the mother cell is
39 almost exhausted, produces fewer daughters with high levels of damaged proteins. In
40 addition, retaining more damage during the early divisions increases the number of healthy
41 daughters in the population.

42

Abbreviations	Description
$RE_{\text{div/dist}}$	Division / distance strategy of damage retention
g	Division number
α, n	repressor activation constant, repressor Hill constant
τ_i, τ_D	Time required for intact/damage component to reach division/ death
I_{div}	Intact component threshold
R_t	Ratio between the times required for division and death threshold
I_g and D_g	Intact and damage component of mother cell after division
re	Damage Retention with altruist effect
re_{max}	Maximum possible damage retention
A	Altruist value to make variation in the strategy
D, D_{death}	Damage variable, Damage threshold
$N_{\text{daugh/mot/pop}}$	Daughter/mother/accumulated cells
$P_{\text{daugh}}, P_{\text{mot}}, P$	Population distribution for daughter/mother/accumulated
$D_{\text{daugh/mot/pop}}$	Damage in daughter/mother/accumulated cells population
$C_{\text{daugh/mot/pop}}$	Cost function for daughter/mother/accumulated cells population

46 **Introduction:**

47 Aging is a conserved scale-invariant phenomenon that exploits entire organism
48 simultaneously, from the organelles involved in the cellular processes to the organs and body
49 structure. Aging factors like damage accumulation and its asymmetric segregation through
50 retention mechanism during growth and division processes respectively have been frequently
51 studied in the past few decades and are proposed to promote ageing from simple unicellular
52 organism like budding yeast to higher eukaryotes (Bufalino et al., 2013; Erjavec et al., 2007;
53 Hill et al., 2016; Katajisto et al., 2015; Kennedy et al., 1994; Kruegel et al., 2011; Zhou et al.,
54 2014). Retention of damage during the process of cell division is an evolutionary conserved
55 mechanism whose efficiency decreases gradually and leads to the senescence state where
56 basic cellular processes are unable to produce enough proteins to have subsequent divisions
57 (Aguilaniu et al, 2003; Ackermann et al., 2003; Erjavec et al., 2008; Rujano et al., 2006).

58 Budding yeast, *Saccharomyces cerevisiae* (*S. cerevisiae*) has been widely studied in aging
59 research and has contributed to the identification of many genes involved in mammalian aging
60 (Longo et al, 2012). Ageing in yeast can be studied by two main approaches: replicative aging,
61 which is measured by the number of divisions that a cell performs before senescence, and
62 chronological aging, which corresponds to the time before a cell enters senescence in a non-
63 dividing state (Longo, 2012). Experiments targeting replicative aging showed that yeast cells
64 give rise to a limited number of daughter cells, usually around 20–25 (Mortimer and Johnson
65 1959, Longo, 2012). Throughout its lifespan, a cell accumulates different types of ageing
66 factors, like extra chromosomal RNA circles (ERCs), increased intracellular oxidative stress,
67 mitochondrial dysfunctions and accumulation of damaged proteins (Aguilaniu 2003, Sinclair
68 1998). It has been shown that asymmetric distribution of damaged proteins in the unicellular
69 organisms is evolutionary beneficial for the whole progeny thus ensuring the highest level of
70 fitness for the daughter cells (Waddington, 1953; Eshel and Matessi, 1998; Crispo, 2007,
71 Kaberlein, 2010). This unequal distribution of damage results in an ageing mother cell and a
72 rejuvenated daughter with full replicative potential (Eglimetz and Jazwinski, 1989). In the early
73 divisions, a mother cell is able to retain most of the damage, giving rise to fully healthy
74 daughter cells. However, in the late stages of a mother cell's lifespan, damage retention
75 becomes less effective, and aging factors begin to be passed to the daughters which, thus, are
76 born prematurely old (Kennedy et al, 1994; Sinclair et al, 1998a; Sinclair et al, 1998b). This

trend reaches a climax in the last 5% of a mother's lifespan when divisions are often symmetric and the daughter inherits a consistent amount of cellular damage from the mother. The gradual decline in the organelles performance during replicative aging results in cells with a unique way of damage retention that is well conserved across natural selection and provide a distinctive reproduction strategy among the different yeast strains (Erjavec et al., 2008; Kirkwood and Rose, 1991; Nyström and Liu, 2014).

From the evolutionary perspective of Darwinism, the variation in the genetic material of a trait is a random process that is passed on to its progeny by means of natural selection. These variations are negligible preserving the structure and function during the lifespan of a particular species (Konieczny et al., 2014). However, there are several characteristics, e.g. age, size and reproduction, which are uniquely identifiable within the same species. Bringing all the characteristics together outlines an evolutionary survival strategy of the population that leads to its reproduction success (Berg et al., 2002; Brooks and Garratt, 2017).

Optimal reproduction success is vaguely understood terminology used to define replicative lifespan of a yeast cell that has evolved the organelles to adapt a finest route for the healthy survival of yeast population. A population's success is in the asymmetric division of cells while keeping the damage low in the progeny and having a long replicative lifespan (Chao et al., 2016; Nyström and Liu, 2014). However, healthy progeny and long replicative lifespan are inversely proportional to each other since it is asserted that, during the replicative lifespan, yeast strains sacrifice their long-term survival over the health of their progeny by retaining the aging factors (Aguilaniu et al., 2003; Hill et al., 2017; Kirkwood and Rose, 1991). Therefore, it is interesting to find a strategy for optimal retention of aging factors in such a way that yeast population accumulates less damage in the living cells and provides maximum population.

Theoretical models have played a critical role in understanding ageing process in the unicellular organisms (Ackermann et al., 2007; Chao, 2010; Chao et al., 2016; Clegg et al., 2014; Coelho et al., 2014; Erjavec et al., 2008; Lindner et al., 2008; Stewart et al., 2005; Vedel et al., 2016). A recent theoretical study has shown that symmetric division alone can lead to a senescence state where cell can no longer divide while some stochastic effects on the damage distribution between mother and daughter cells can protect cells from early damage (Chao et al., 2016). Moreover, the natural selection adapts the protective mechanism into the

subsequent progeny in a genetically controlled manner. The asymmetric division in yeast cells increases the population fitness in case of high damage propagation rates and therefore increases the proliferating capacity of the progeny (Erjavec et al., 2008). It has been suggested that the optimal aging strategy is to repair the transcriptional errors and mal-functionalities by recycling the damaged material to maintain the quality rather than segregating the damaged portions (Clegg et al., 2014). However, the protein quality control system is not sufficiently effective to maintain the proteostasis and therefore cellular health is sacrificed over the continuous production of proteins (Nyström and Liu, 2014; Orgel, 1963). Therefore, the segregation of damaged proteins in spatially sequester regions of a cell becomes a necessity in order to maintain the performance of the organelles involved in the fundamental cellular processes (Hill et al., 2017; Tyedmers et al., 2010).

In previously computational models, retention of damage is, **due to simplicity**, assumed to have the same efficiency throughout the cells replicative life, thus it is treated as a constant (Erjavec et al., 2008; Clegg et al., 2014). Here, **based on several experimental evidences reported in yeast (Kennedy et al, 1994; Sinclair et al, 1998a; Sinclair et al, 1998b)**, we consider that damage retention, like many other processes, loses its efficiency during the replicative lifespan of yeast cell. However, the exact mechanisms of damage retention still remain unclear. We propose two strategies named as *distance strategy* and *division strategy*, to investigate the efficiency and stability of damage retention during the replicative lifespan of single cell. We ask whether it be possible that any two yeast strains following different strategies of damage retention converge to a unique optimal reproduction success. We also investigate whether a yeast population following a well-defined strategy of damage retention reaches a specific optimal reproduction success that her fellow mutated species cannot reach until it follows the same strategy.

Mathematical Modelling

Mathematical model **presented here is built on a model published by Erjavec et al, 2008** and comprises of division and growth processes for each cell using discrete-continuous model (Appendix 1). Each cell increases its intact and damaged components during the growth process and asymmetrically distributes these components between the dividing cells (mother and daughter cells) during the division process. The damage retention mechanism allows

mother cell to retain part of the damage proteins from the daughter cell and, in return, give part of the intact portion. The efficiency of damage retention decreases during the whole replicative lifespan in a specified manner, termed as strategy of premiere cell. This strategy is followed by the cell and its whole progeny during their respective replicative lifespans. A pedigree-tree model follows the whole population and provides a discrete population distribution function over the damaged component.

In this work, we consider, two yeast strains following distinct strategies of decreased efficiency of damage retention during the cell division. These strategies are based on the assumption that each strain is tuned for a long replicative lifespan and not for its own long-term survival (Kirkwood and Rose, 1991; Nyström and Liu, 2014). Small variations in a strategy are implanted to alter the way of decreasing the efficiency of damage retention. It is considered that each variation in the strategy represents an altruistic behaviour of a mother cell for her progeny. However, for each variation, whole pedigree-tree model is simulated and cost functions are calculated. These cost functions are based on the damage proportion of the alive cells and their population size.

Damage retention strategies

Retention parameter can be varied considerably in multiple ways while each one can provide a significant effect on the population in the long run. However, it is not feasible to follow all plausible ways of reducing the efficiency of damage retentions due to computational limits. Therefore, it is inevitable to develop strategies by means of well-defined functions for the efficiency of damage retention. Two strategies, named as *division strategy* and *distance strategy*, are defined to investigate the efficiency of damage retention during the replicative lifespan of single cell. Strategies have been developed in such a way that a mother cell following distance strategy retains more damage than a mother cell following division strategy during the early divisions.

Division Strategy

In a division strategy we define retention efficiency as a repressor Hill function in the following way

$$RE_{div}(g + 1) = 1 - \frac{g^n}{g^n + \alpha^n} \quad (1)$$

where $\alpha > 0$ and $n \geq 1$ are constants. Increasing these constant values can slow down the decrease in the efficiency of damage retention in the subsequent divisions of the mother cell (Figure 1).

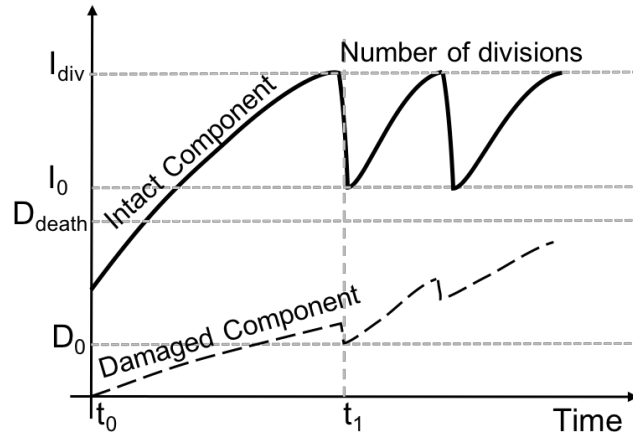


Figure 1: Division strategy: Efficiency in damage retention decreases with the increase in number of divisions. Mother cell is able to retain maximum damage in the beginning but loses its efficiency of damage retention as the number of divisions increases. The intact component decreases from its threshold I_{div} to $I_{g=0}$ after division and the damaged component decreases to $D_{g=0}$. The cell death threshold is represented by D_{death} .

Distance Strategy

In distance strategy the efficiency of retaining damage (RE) decreases with the increase in the number of cell divisions and is also modelled by repressor Hill function as:

$$RE_{dist}(g + 1) = 1 - \frac{R_t^n(g)}{R_t^n(g) + \alpha^n} \quad (2)$$

The parameters $n > 1$ and $\alpha > 0$ can be set according to the R_t value; however, these parameters are the same as in the previous strategy (see Appendix 1). The variable R_t is the ratio between the time required for intact component to reach division level (τ_i) and the time required for damage component to reach cell death (τ_D).

$$R_t = \frac{\tau_I}{\tau_D} \quad (3)$$

Due to the increase in damage during the replicative lifespan of a cell, the retention becomes more difficult. After every division cell anticipates the possibility of next division. If the damage is high enough such that next division is not possible then cell further decreases its retention to the minimum level ($RE_{\text{dist}} = 0$) as in the division strategy. The required times (τ_I and τ_D) are calculated by taking ratio between remaining distance and the mean rate of change in the corresponding intact ($Avg(\dot{I})$) and damage ($Avg(\dot{D})$) component.

$$\tau_I = \frac{I_{\text{div}} - I_g}{Avg(\dot{I})}, \tau_D = \frac{D_{\text{death}} - D_g}{Avg(\dot{D})} \quad (4)$$

In the distance strategy (Figure 2), cell composition is divided into two components which are increasing during their growth process. The increase in the damage component is represented by long-dashed lines (— —) that starts from zero and passes through D_0 and intact component by continuous lines that starts from minimum amount of intact proteins. At time t_1 , the cell reaches the division threshold (I_{div}) where it is ready to bud a daughter with asymmetric distribution of intact and damage component. After division, mother cell has intact component I_g and damage component D_g . At this point the distance strategy comes into action. The parametric value of retention set by the strategy is used to anticipate the success in completing next division by the above defined procedure (see Eq. 2). If the next division is possible then the cell will divide according to the defined strategy. Otherwise the cell will decrease the retention to its minimum value so that next division becomes possible.

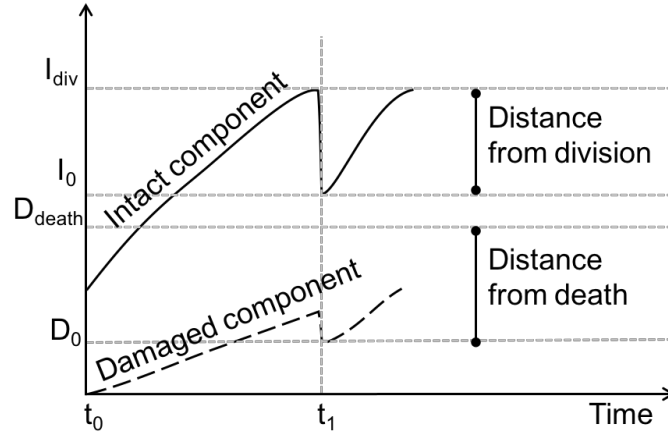


Figure 2: Mother cell decreases damage retention by anticipating her next reproduction success. Cell increases its initial intact and damage component from t_0 and divides at time t_1 . The intact component decreases from its threshold I_{div} to $I_{g=0}$ after division and the damaged component decreases to $D_{g=0}$. The cell death threshold is represented by D_{death} .

Altruistic Variation in the Efficiency of Damage Retention

The strategies provide a unique way of decreasing the efficiency of damage retention which can be varied by using an altruist factor (A) as defined in Eq. (5). The parameter A is based on the consequences of the actions performed for replicative lifespan of a mother cell and for reproductive fitness of the offspring that is measured by determining their health status. The parameter $A = 0.5$ is defined as a neutral value when it has no effect on the strategies of damage retention and therefore follows the asymmetric division as defined in Eqs. (1) and (2). For $A < 0.5$, cells show selfish behaviour to their progeny by retaining less damage than being neutral during their replicative lifespan, whereas for $A > 0.5$, cells show selfless behaviour by retaining more damage than the one defined in a neutral strategy. At the extreme values, the cells show either no retention ($re = 0$) or full retention ($re = 1$) during their replicative lifespan.

At the time of division, damage retention is set in two stages. Firstly, $RE(g)$ is calculated by means of defined strategy (distance or division strategy). Secondly, altruism parameter is used to alter the strategy. At the moment when no more divisions are possible, the retention decreases to zero allowing another division without taking the altruist effect into account. The equation for altruist retention is written as:

$$re(A, g) = RE(g) + 2 \left(A - \frac{1}{2} \right) ((1 - A)RE(g) + A(re_{max} - RE(g))) \quad (5)$$

214 The parameter re is altruism-dependent efficiency of damage retention and re_{\max} is the
215 maximum attainable retention, i.e. 1.

216 **Pedigree-tree model**

217 Here we develop a pedigree-tree model to follow complete population with variable retention
218 parameter (Appendix 1). The cellular growth is represented by increase in the number of intact
219 and damage components and the division is represented by asymmetric distribution of growth
220 components (intact and damage) between mother and daughter cells. Advantage of this
221 model is that the cells are instantly counted when bud out from their mothers while their
222 growth components are tracked throughout their replicative lifespan. At the end of
223 simulation, the cells are distributed according to their intact and damage components in a
224 discrete manner. Moreover, the variable retention of a single cell during its lifespan can be
225 applied over the whole population in an appropriate manner. Following this procedure leads
226 us to find the population distribution function for damage component and to investigate the
227 differences between strategies by using cost functions.

228 **Population distribution function for intact/damage component**

229 Each cell is born with a specific level of damage and intact components and grows accordingly
230 until it reaches division threshold that leads to its asymmetric binary division. The division
231 leads to a new daughter cell which follows the same growth and division strategy as her
232 mother. During this process the population increases, generating cells with diverse level of
233 intact/damage components. These components can be distributed over the whole population
234 at any time $t = t_0$ and can be represented by a population distribution function $P(A, D)$.
235 Therefore, for each altruist value A and accumulated damage D , the population distribution
236 function for damaged component is written as,

$$P(A, D) = \frac{\sum_{D=a}^{D=b} (N_{daugh}(A, D) + N_{mot}(A, D))}{N_{pop}(A)}. \quad (6)$$

237 where a and b are the minimum and maximum accumulated damage. The functions $N_{daugh}(A,$
238 $D)$ and $N_{mot}(A, D)$ represent the number of daughter and mother cells with $D \in [0, D_{\text{death}}]$

amount of damage component at a given altruist value A . The population distribution function is normalized by total population of alive cells $N_{\text{pop}}(A) = \sum (N_{\text{daugh}}(A, D) + N_{\text{mot}}(A, D))$. The variation in N_{pop} due to altruism A is well-intended to ensure the total size of the population at any time $t = t_0$. Similar kind of distribution functions can be defined for the normalized population distribution of daughter cells, $P_{\text{daugh}}(A, D)$, and mother cells, $P_{\text{mot}}(A, D)$ as follows:

$$P_{\text{mot}}(A, D) = \frac{\sum_{D=a}^{D=b} N_{\text{mot}}(A, D)}{\sum_D N_{\text{mot}}(A, D)},$$

$$P_{\text{daugh}}(A, D) = \frac{\sum_{D=a}^{D=b} N_{\text{daugh}}(A, D)}{\sum_D N_{\text{daugh}}(A, D)}.$$
(7)

Cost Functions

The calculation of cost function is performed at the end of discrete-continuous model while the objective is to find the minimum cost function so that smallest amount of damage and maximum number of cells exist in the population. The damaged component and the total population is calculated for the virgin cells – the cells that have not undergone any division yet, for the mother cells and for the whole population. These calculations are then normalized, defined by $\tilde{N}(X)$, where X is any population distribution of either mother, daughter or total cells with a given altruist value and damage D . This helps to eliminate the redundancy between the cellular components and the population. $\tilde{N}(X)$ can be defined as,

$$\tilde{N}(X) = \frac{X - X_{\min}}{X_{\max} - X_{\min}}$$

The normalization is carried out by finding the extreme values from the deterministic model for the total damage in the cells and the total population. The extreme values for each cost function exist at unique values of altruism $A \in [0,1]$.

Cost function at any given altruism value A in case of daughter cells is the sum of normalized accumulated damage of all the daughter cells, $\tilde{N}(\sum_{D_{\text{daugh}}} D_{\text{daugh}}(A))$, and difference between normalized maximum number of daughter cells during $A \in [0,1]$, i.e. equals to 1, and normalized alive daughter cells, $\tilde{N}(N_{\text{daugh}}(A, D))$, present in the system at any time $t = t_0$.

$$C_{daugh}(A) = \tilde{N} \left(\sum_{D_{daugh}} D_{daugh}(A) \right) + \left(1 - \tilde{N} \left(\sum_D N_{daugh}(A, D) \right) \right) \quad (8)$$

261 The cost function for damage component in the mother cells at a given value of A is similar to
 262 the cost function defined for damage component in the daughter cells. The only difference is
 263 that we calculate damage in those cells that have been divided at least once. We write this
 264 cost function as,

$$C_{mot}(A) = \tilde{N} \left(\sum_{D_{mot}} D_{mot}(A) \right) + \left(1 - \tilde{N} \left(\sum_D N_{mot}(A, D) \right) \right) \quad (9)$$

265 Damage in a mother cell is denoted by D_{mot} and total population of the mother cells is N_{mot} .
 266 For the damage proportion in the total yeast population at a given altruism A , $N_{pop}(A)$, the cost
 267 function is the sum of the normalized damage in the total population, $\tilde{N}(D_{pop})$, and the
 268 difference between the normalized maximum and the normalized current population sizes,
 269 i.e. $1 - \tilde{N}(N_{pop})$. It is given by the following formula,

$$C_{pop}(A) = \tilde{N} \left(\sum_{D_{pop}} D_{pop}(A) \right) + \left(1 - \tilde{N}(N_{pop}(A)) \right) \quad (10)$$

270 Variation in Altruism

271 Altruism parameter A is varied deterministically as well as stochastically. The deterministic
 272 way is quite straight forward as it formulates the normalized distribution of cells at discrete
 273 values of A and calculate cost functions for each value of A that varies in the interval $[0,1]$.
 274 These cost functions are further used in the stochastic model to help find the minimum value
 275 of cost function.

276 The stochastic settings involve individual based modelling approach in which altruist
 277 parameter A is randomly chosen from its neighbouring values. Small variations bring changes

in the strategy of damage retention and mimic the concept of mutation which directly affects the cost function. The cost of following an individual's strategy of damage retention by its progeny is deterministically calculated by using Eqs. (8), (9) and (10) which involves simulation of pedigree-tree model for a specific period of time. The method allows the cell to follow the direction where it finds minimum cost function. The direction of the altruist value is chosen on the basis of current and preceding cost functions by using the signum function while the magnitude of the variation is set by choosing random value in the interval of $[0, \varepsilon]$.

$$A_{i+1} = A_i \pm \text{rand}(0, \varepsilon) \text{sgn}(C(A_{i-1}) - C(A_i)) \quad (11)$$

This process continues for a set period of time and is terminated by the following criteria,

$$\sum_{i=S_N+l}^{S_N+j+l} |A_{i-j} - A_{i-(j+k)}| < \varepsilon. \quad (12)$$

In the above equation, sign \pm are set according to the direction of altruist value and the index of altruism A indicates the strategy variation number. The positive sign is used when direction of altruism is upward, i.e. $A_{i-1} < A_i$, whereas the negative sign is used in case altruism is decreasing, i.e. $A_{i-1} > A_i$.

Results:

Initially, there is a single daughter yeast cell present in the system that has sufficient amount of intact proteins to grow and doesn't contain any damaged proteins. A general behaviour of the model is described in Figure S1.

In the course of this work we sought to establish relationship between strategies followed by distinct yeast strains and relationship among yeast strains following the same strategy. The former is followed deterministically to find the reproduction success by using the given cost functions whereas in the later the optimality is investigated by making stochastic variations in the strategies.

299 **Relation Between Strategies**

300 Damage retention strategies follow a defined way to decrease the retention efficiency of a
301 mother cell. However, there are unique routes associated to each value of altruism that are
302 followed according to their intrinsic behaviour represented by Eqs. (1) and (2). The distance
303 strategy keeps the damage retention high and decreases the efficiency at an increasing rate
304 whereas the division strategy was defined in an opposite fashion by showing a sharp decrease
305 during the early replicative lifespan of a mother cell.

306 The strategies are defined using Hill function in the equations (1) and (2) with $\alpha = 1$ (Figure
307 3). A comparison between the symmetric and asymmetric cell divisions has been performed
308 to observe the effect of strategies over the number of divisions while choosing different sizes
309 of the cells. The variations in the strategies is given by altruist parameter A with $A_{max} = 1$. It is
310 interesting to note that both strategies provide same behaviour at the end points of A , i.e. 0
311 and 1 (Figure 3).

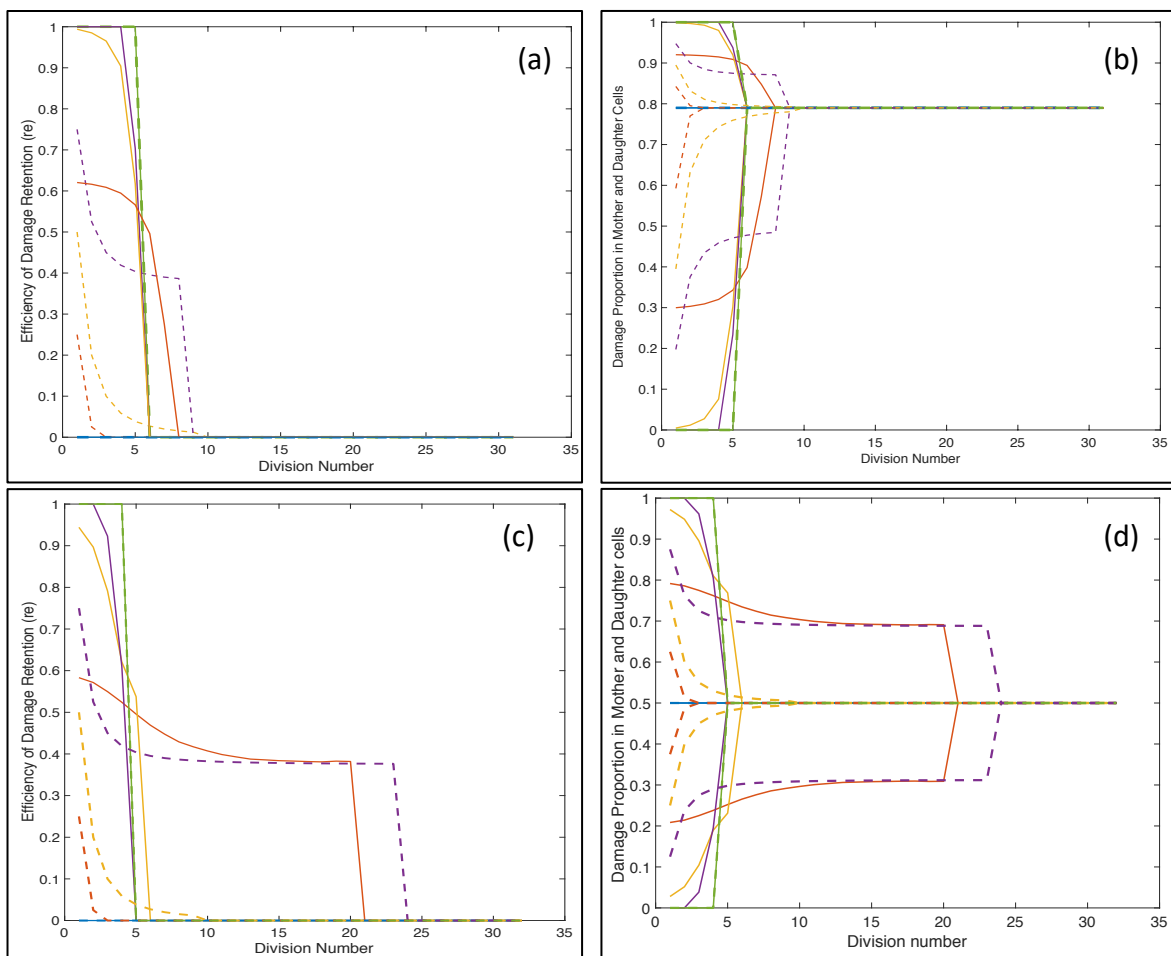


Figure 3: Damage retention efficiency (RE) for altruist parameter values $A = 0$ (blue), 0.25 (red), 0.5 (yellow), 0.75 (violet) and 1 (green). The dashed lines represent division strategy and continuous lines represent distance strategy. Colours are drawn to match the altruist parameter values between the two strategies. Left hand side panels (a) and (c) shows the damage retention by mother cell while the right-hand side panels (b) and (d) are obtained by relating size-wise damage distribution among mother and daughter cells. The cell sizes after division of cells are chosen asymmetric ($R_m = 0.79$) for panel (a) and (b) and symmetric ($R_m = 0.5$) for panel (c) and (d).

At $A = 0$, yeast cell does not retain any damaged portion ($re(0, g) = 0$) during its replicative lifespan and therefore share damage with her daughter according to the division size of the cell R_m . Consequently, yeast survives for a longer replicative time and buds off 31 daughters when $R_m = 0.5$ and 32 daughters when $R_m = 0.79$ (Figure 3). On the other hand, at $A = 1$, yeast cell retains all the damage ($re(1, g) = 1$) and buds a completely healthy daughter cell each time which affects its lifespan and brings it to 5 divisions. For all the other altruist values, i.e. $0 < A < 1$, A does not provide same retention function for both strategies. It can be observed

that cell with division strategy retains less damage than distance strategy; however, the former retains damage for a longer period of time during its lifespan. After the critical damage level when no more retention possible, the cell loses all the retention and share the damage according to the cell sizes.

Population Distribution of Damaged Proteins

The pedigree-tree model provides large population of cells where intact and damage components are individually tracked throughout their replicative lifespan. This provides a non-uniform distribution of alive cells over damaged components. Therefore, the cell population is clustered according to the accumulated damage in each cell (with cluster size of 60 and number of clusters of 10 in the interval $[0, 600]$) for five values of altruism $A = 0, 0.25, 0.5, 0.75$ and 1 (Figure 4, Figure 5 and Figure 6). The maximum attainable damage is bounded by the threshold $D_{\text{death}} = 600$; however, the figures show that the cell could have accumulated damage at most in the interval $[480, 540)$. These clustered populations are normalized in order to calculate the proportion of cells with respect to the total population. Moreover, the error bars are drawn to find the mean and standard deviation of the proportion of cells attaining specific proportion of accumulated damage at the four simulation times $t = 1.5, 1.75, 2$ and 2.25 .

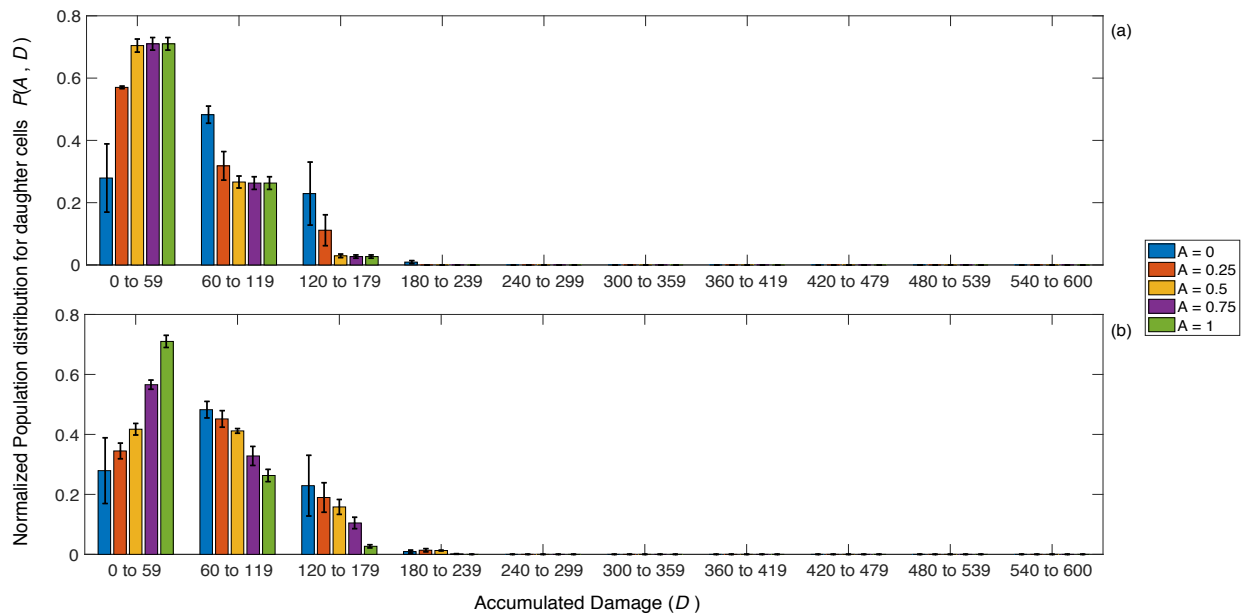


Figure 4: Mean and standard deviation of the daughter distribution of damaged proteins by using distance (a) and division (b) strategies, see Eq. (7). Mean of the distribution is taken for the simulation

time $t = 1.5, 1.75, 2, 2.25$. The accumulated damage in the span of 600 is clustered into subintervals each of length 60.

The population distribution of daughter cells is present only in the first three clusters of damage component (Figure 4). In the first cluster, $D_{\text{daugh}} \in [0, 59]$, mean proportion of cells, $P(A, D)$, increases when altruism A goes from 0 to 1 while the succeeding clusters show a reverse behaviour. The error bars represent the standard deviation of the mean distribution values for simulation time $t = 1.5, 1.75, 2, 2.25$. For $A = 0$, the standard deviation is quite high because the cell proportion was higher in the first and third clusters ($P(A = 0, D = [0, 60]) \approx 0.38$) during the early simulation time, $t = 1.5$. However, it decreased to below 0.2 in the later simulation time, $t = 2.25$. Moreover, for $A \geq 0.5$, the proportion of cells with least damage is much high and have a very small standard deviation.

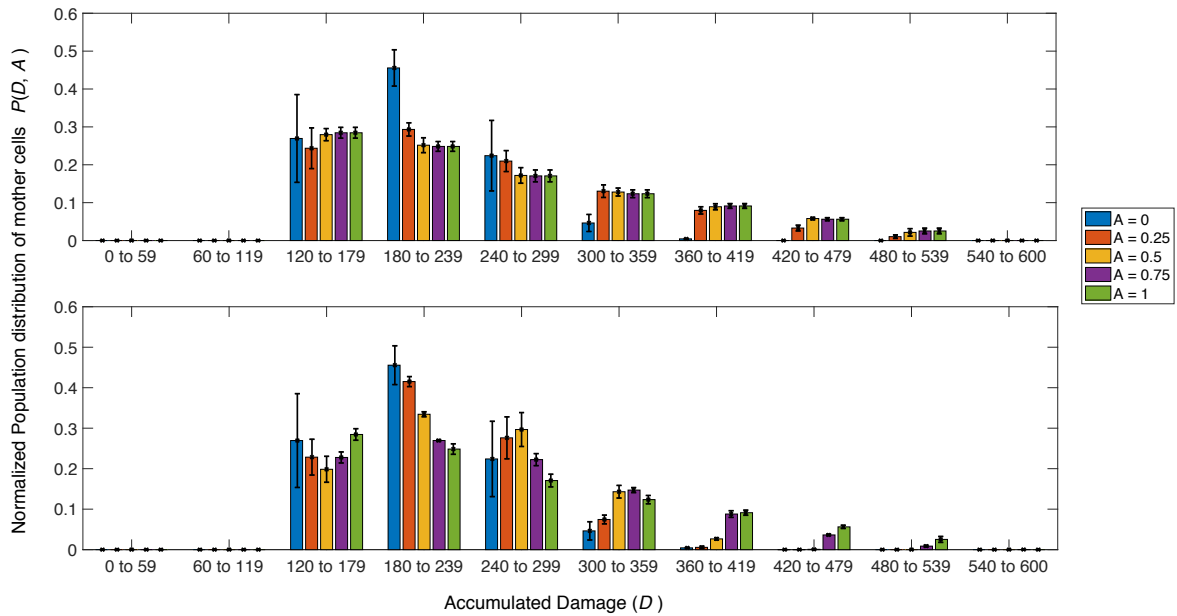


Figure 5: Mean and standard deviation of the mother distribution of damage proteins by using distance (a) and division (b) strategies, see Eq. (7). Mean of the distribution is taken for the simulation time $t = 1.5, 1.75, 2, 2.25$. The accumulated damage in the span of 600 is clustered into subintervals each of length 60.

The number of daughter cells gradually increases in the first cluster of accumulated damage as A goes from 0 to 1 however it shows opposite behaviour in the second and third cluster (Figure 4b). It can be observed that the mean proportion of daughter cells following the distance strategy is higher than the mean proportion following the division strategy in the first cluster for all values of A , except the extreme values where both strategies provide same result. However, the behaviour is opposite in the next two clusters. This suggests that the

distance strategy, i.e. keeping the retention high in the early divisions, accumulates less damage in the population.

Mother cells distribution for damaged component is also normalized and its mean and standard deviation is calculated for the given simulation times $t = 1.5, 1.75, 2$ and 2.25 and altruism values $A = (0, 0.25, 0.5, 0.75, 1)$ and accumulated damage component in mother cells is shown in the third and succeeding clusters (*Figure 5*). This means that cells become mother in the third cluster of damage accumulation however the highest proportion of cells are present in the fourth cluster where damage is in the interval $[180, 240)$. The standard deviation of the mean proportion of mother cells is similar to the mean proportion of daughter cells and therefore cellular health becomes better as A goes from 0 to 1. In comparison between the two strategies, the mothers following the distance strategy have higher damage than mothers following division strategy. In addition, the mean proportion of mother cells containing high damage is comparatively lower than the ones containing low damage.

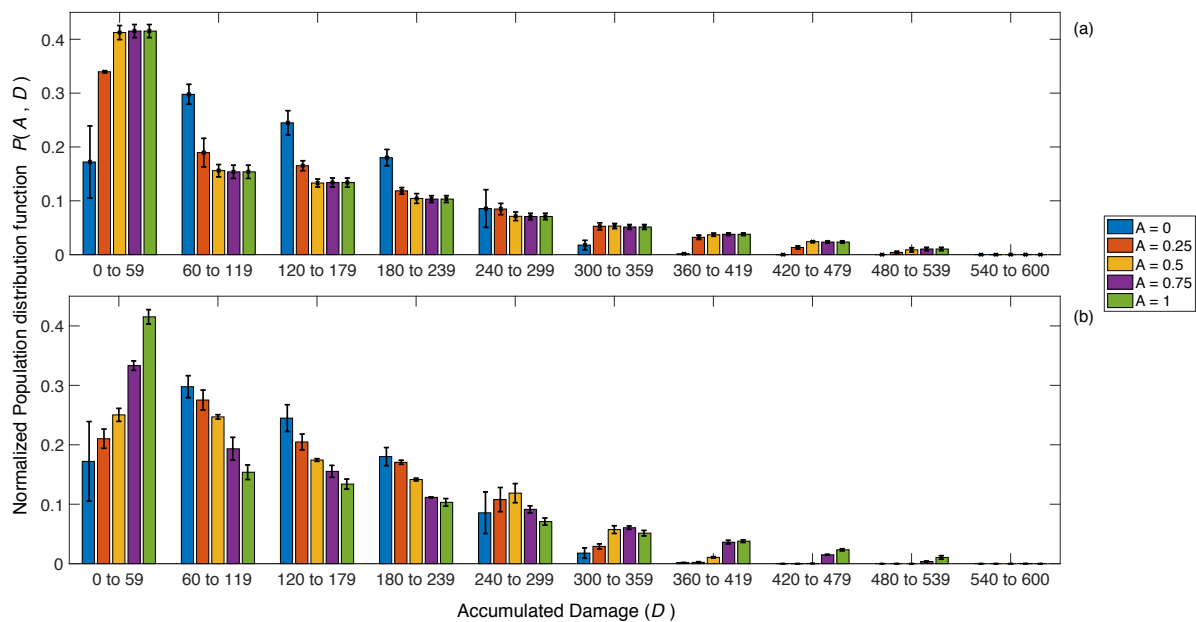


Figure 6: Mean and standard deviation of the normalized population distribution of damaged proteins by using (a) distance and (b) division strategies as defined in Eq. (6). Mean of the distribution is taken for the simulation time $t = 1.5, 1.75, 2, 2.25$. The accumulated damage in the span of 600 is clustered into subintervals each of length 60.

Mean and standard deviation of the normalized distribution of cells over the accumulated damage in alive cells show the behaviour similar to the above distributions at different values of A , however there is a significant decline in the proportion of healthy cells, i.e. first cluster

(Figure 6). At $A = 0$, the standard deviation gives comparatively high values. This is due to the fact that premier cells do not have enough damage to share with their daughter cells for short time scale ($t = 1.5$) and therefore most of the daughter cells born with damage are grouped in clusters 1 and 2. Moreover, the proportion of cells is significantly decreased to below 0.2 when time duration is increased to $t = 2.25$.

Optimal Reproduction success

Models are simulated in deterministic as well as stochastic settings to find the cost functions. These cost functions represent reproduction success by taking into account the cellular health status and population size. The deterministic model provides cost for predefined values of altruism A whereas the stochastic model tracks the minimum value for cost function by taking random steps towards the lowest value of the cost function.

Deterministic outcomes

Deterministic modelling approach is used to evaluate the cost functions by varying the altruist parameter A between 0 and 1 with the step size $\Delta A = 10^{-3}$. The results are obtained for the cost functions defined in Eqs. (8), (9) and (10) and are presented in Figure 7 (for daughter cells), in Figure 8 (for mother cells) and in Figure 9 (for total number of alive cells) respectively each at four different times $t = 1.5, 1.75, 2$ and 2.25 . **Computationally, it becomes very expensive to go beyond time point $t = 2.25$. Therefore, this is the maximum time point chosen. Other time points are chosen to understand the behaviour of cost function over the altruism parameter A .** The cost function is modelled by taking this fact into consideration that the replicative lifespan decreases with the increase in damage retention by the cell. In such scenario, it would be interesting to see the effect of replicative lifespan over the damage accumulation in the population.

Altruistic effects on the daughter cells provide a time variant response to its cost function. Due to asymmetric division, mother cells require less time to reproduce than the daughter cells. Therefore, longer lifespan of mother cells will quickly increase the population; however, in case of low damage retention, high amount of damage is passed on to the newly born daughter cells. In case of distance strategy, this phenomenon quickly increases the damage in the population and raises the cost function to high level during the early time, i.e. $t = 1.5$ and

1.75 (Figure 7, Figure 8 and Figure 9). However, with the progression of time, i.e. t goes to 2 and 2.25, the cost function gives a surprising outcome by replacing the high values with the lower ones, exposing that for large time scale, population size can dominate over the total damage present in the population. For instance, the distance strategy (continuous lines) near $A = 0.3$, the cost function that was at maximum, i.e. $C_{\text{daugh}} = 1.2$ at time $t = 1.5$, goes below the value of $C_{\text{daugh}} = 1$ at time $t = 2.25$.

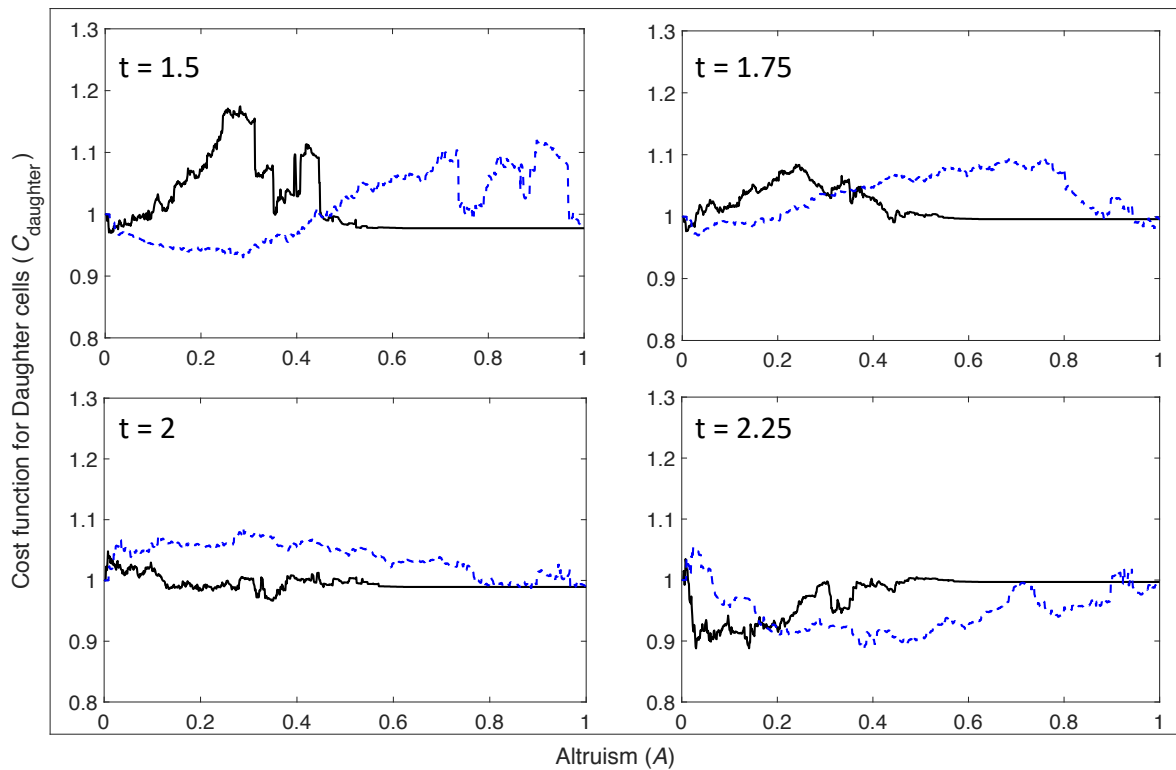


Figure 7: Cost function for the distance (continuous lines) and division (dashed lines) strategies of daughter cells C_{Daugh} at four time-points $t = 1.5, 1.75, 2$ and 2.25 against the altruist values A in the interval $[0,1]$ and step size 0.001 . Cost function is defined in Eq. (8) while the deterministic model used to simulate the results is described in the Appendix 1.

Division strategy provides opposite response than the distance strategy during the early simulation time by showing a small decrease in the payoff function for early altruism values. The reason is clearly that the proportion of cells in the population decreases slightly slower than the increase in the proportion of damage accumulation (

429

430

431

432

433

434

435 *Figure S4: Proportion of daughter cells and their damage in the population for time $t = 1.5, 1.75, 2$ and 2.25 . The*
436 *continuous lines represent distance strategy while dashed lines represent division strategy. The lines moving from*
437 *0 to 1 are the daughter cells proportion while the lines moving from 1 to 0 are the damage proportion.*

438

439

440

441

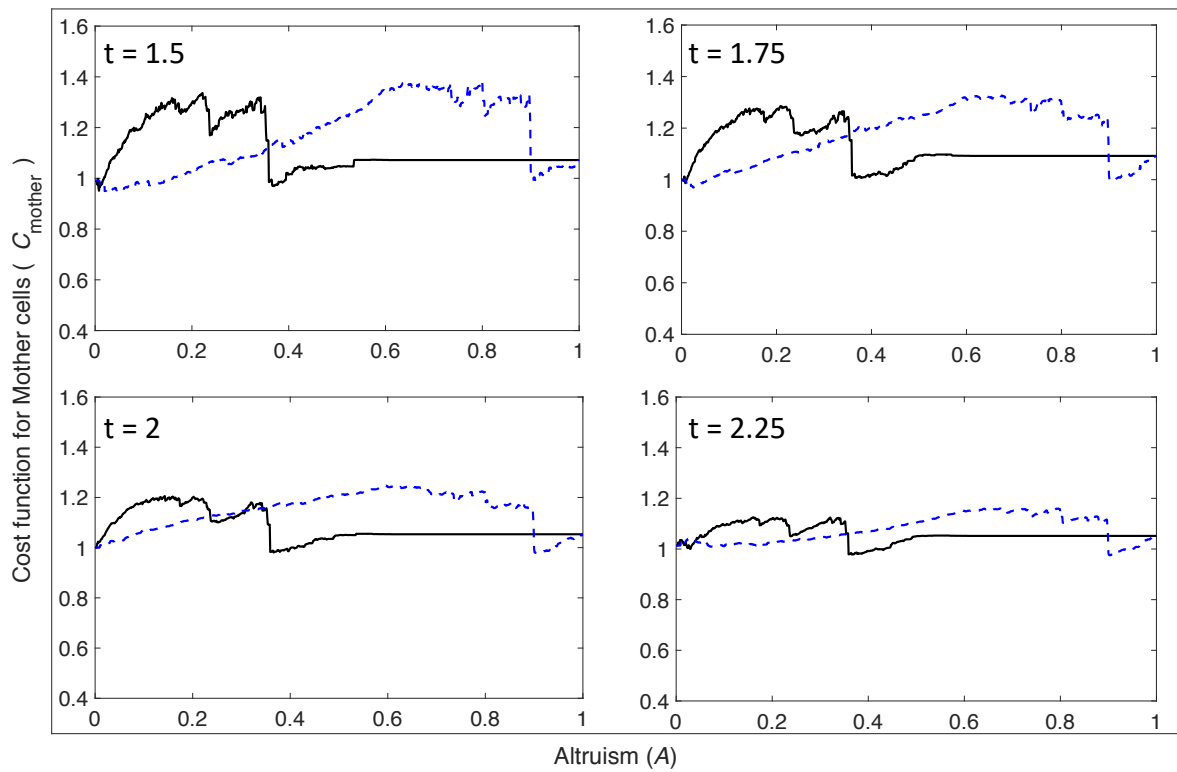
442

443

444

445). For longer period of time, $t = 2.25$, both strategies decrease their cost function for early
446 values of A , however, their optimal reproduction success varies.

447



448 Figure 8: Cost function for the distance (continuous lines) and division (dashed lines) strategies
449 of mother cells C_{Mot} at four time-points $t = 1.5, 1.75, 2$ and 2.25 against the altruist values A in
450 the interval $[0,1]$ and step size 0.001.

Taking the final time into consideration, the results provide several interesting outcomes regarding the least value for the cost function, i.e. the optimal reproduction success. First of all, the optimal reproduction success for both strategies require selfish behaviour of mother cells when altruism parameter $A < 0.5$. However, a complete selfish behaviour is not a good strategy which may increase the damage in the population. It is also worth enough to mention here that the cost function varies significantly from one simulation time to the next one, e.g. $t = 2$ to 2.25 which means that the cost function is not in an equilibrium state. Conversely, it is interesting to note that the cost function is squeezing around $C_{\text{Daugh/Mot/Tot}} = 1$ by reducing the drastic changes. These drastic changes cause fluctuations in the cost function whose local minimum is termed as “evolutionary ditch”. These ditches may not provide the least cost function; however, it becomes difficult to come out from such ditches since these are surrounded by high values of cost functions.

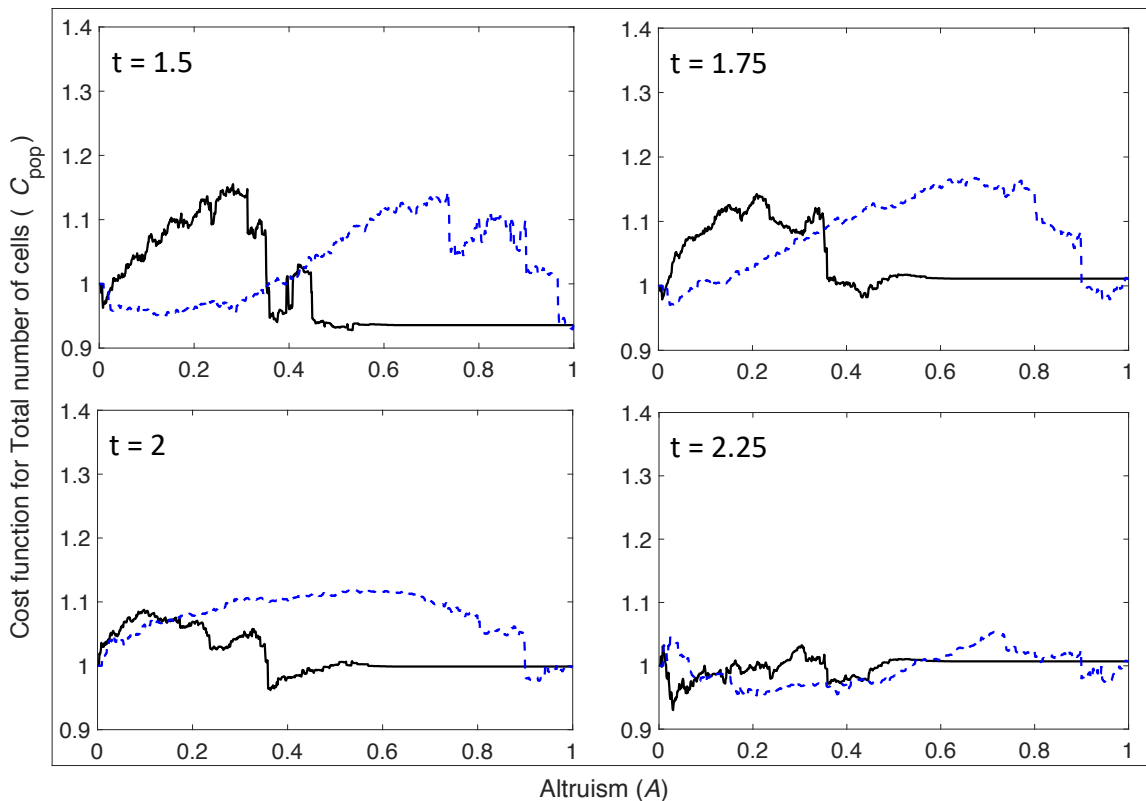


Figure 9: Cost function for the distance (continuous lines) and division (dashed lines) strategies of total cells C_{pop} at four time-points $t = 1.5, 1.75, 2$ and 2.25 against the altruist values A in the interval $[0,1]$ and step size 0.001 .

467 Stochastic Simulations

468 Stochastic settings are implemented to observe the behaviour of cost function for total cells
469 calculated at the simulation time $t = 1.5$. The strategies starting points are chosen for altruist
470 values A between 0 and 1 with a step size of 0.1 (*Figure 10*). At each altruist value, cost functions
471 are calculated which are then compared to their previous values. The strategies vary in the
472 direction where small values of cost function are found by using Eq. (11). However, the least
473 value is not predefined in the stochastic settings and therefore the simulation continues even
474 after reaching the least cost function. The cost function is very sensitive in the sense that a
475 small variation in altruist parameter can vary the yeast efficiency of retaining damage which
476 may result in the decrease/increase in the yeast cell population and damage accumulation in
477 the population. This fallouts fluctuation in the cost function which sets the direction by varying
478 altruism values as shown in the *Figure 10*. In the simulations, an important aspect to analyse is
479 that most of the fluctuations occurred at some specific altruism values. The stopping criteria
480 is implemented after 1000 variations, strategy variation number (S_N) = 1000, **by the following**
481 **inequality**

$$\sum_{i=S_N+l}^{S_N+j+l} |A_{i-j} - A_{i-(j+k)}| < \varepsilon \quad (12)$$

482 The index values are $j = k = 10$ and the epsilon $\varepsilon = 0.02$. The parameter epsilon provides the
483 maximum possible variation in the altriusm value and is used in the Eq. (11). The stopping
484 criteria is defined by the summation expression that stops the simulation if the ε condition is
485 fulfilled consecutively for five values of index l .

486 The altruist effects on distance strategy (*Figure 10a*), have revealed clear differences between
487 the values of A chosen above and below the neutral one, i.e. 0.5. For a yeast population
488 following its strategy with altruism $A \geq 0.5$, the cost function decreases as A increases and
489 eventually A reaches to the maximum value. On the other hand, when $A < 0.5$, the strategy
490 varies most of the time around the values $A = 0$ and 0.4 that are surrounded by evolutionary
491 ditches. Since strategies are tuned to keep varying A in the direction where least value of cost
492 function (minimum of cost function) is found, therefore, the sensitivity in cost function against

the altruist values allows cells to alter their strategy which creates a safe escape from the evolutionary ditch. In a similar way, these strategies escape from the least values of the cost function. Such escapes are made possible due to the involvement of randomness in the altruism.

The division strategy also shows similar behaviour as distance strategy however the strategy is more frequently observed around the extreme values of altruism, i.e. $A = 0, 0.1, 0.9$ and 1 (Figure 10b). The simulations show that strategy started around $A \leq 0.4$ could not escape from the local minimum of the cost function while the starting value of A above 0.8 eventually reached to their evolutionary ditch.

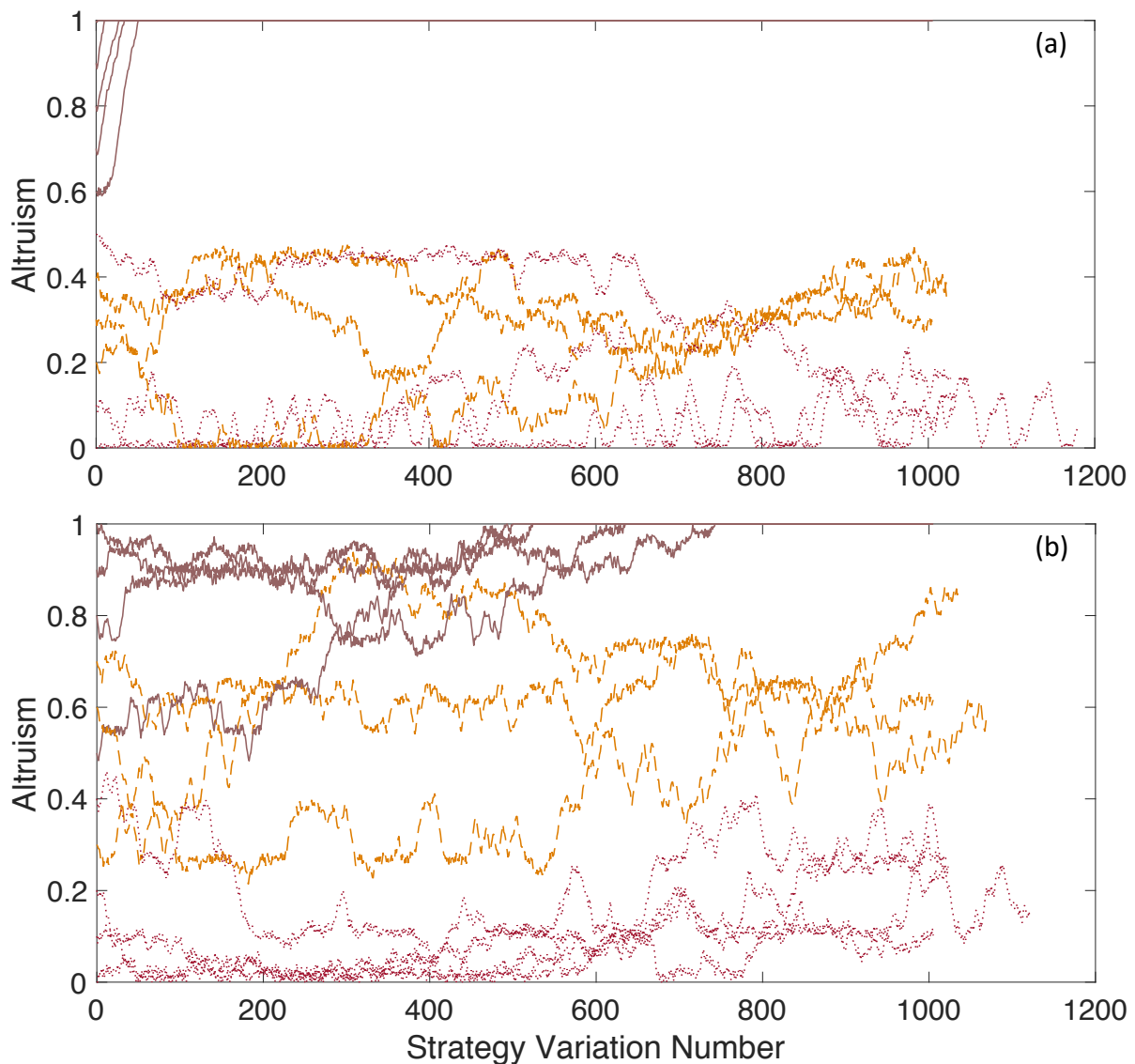


Figure 10: Stochastic simulations of (a) distance and (b) division strategies at time $t = 1.5$. The altruism parameter A is varied randomly for each strategy variation number in the interval $[0, \varepsilon = 0.02]$. The lines styles are used to clear up the tracking of each simulation.

505 **Conclusions**

506 Efficiency of damage retention provides a monotonically decreasing function in which mother
507 cell retains lower amounts of damage in each subsequent division. The defined strategies have
508 provided unique ways for decreasing the efficiency during cell replicative lifespan of a budding
509 yeast while the altruism factor was used to make deviations in the strategy. For each
510 deviation, a well-defined cost function is computed. Deterministic settings were adopted to
511 analyse the behaviour of cost functions for each strategy. It has also provided the extreme
512 values of the cost function which were further used under the stochastic settings. The cost
513 functions were varied by means of random altruistic effects given to the strategies. These
514 variations were tuned to find the optimal reproduction success of population. However, the
515 strategies that started at different altruist values, ended up optimizing in a local fashion rather
516 than approaching a global minima of cost function.

517 **Distance vs Division Strategy**

518 Our results showed that retaining more damage in the beginning provides healthy daughter
519 cells which plays a significant role in maintaining accumulated health of the population.
520 Moreover, the daughters born with high damage did not replicate as often as daughters born
521 with low damage. In case of division strategy, the mother cell shared more damage in the
522 early divisions, leading to poor health of progeny. At the later stage of replication, when the
523 damage efficiency is low, the mother cell shared high level of damage with its daughter cells.
524 Consequently, these daughter cells could not provide healthy progeny to the population.

525 **Altruism Provides Healthy but a Small Population**

526 Increase in the altruist values increases the efficiency of damage retention of the mother cell.
527 A complete altruist behaviour allows a mother cell to retain all the damage at the time of
528 division which reduces its replicative lifespan while giving birth to completely healthy
529 daughter cells (Figure 3). In case of whole pedigree, the same phenomenon is followed
530 (Figures S1). When both factors, health and population size are considered (Figures 7 – 9), the
531 cost functions of each strategy provided different global minima, while the distance strategy
532 provides lower cost than the division strategy. This shows that a yeast following division

533 strategy can never achieve a better health and population status than a yeast following a
534 distance strategy.

535 Population size and population health have shown reverse behaviours. Increasing population
536 size affects the health of the population and brings more damage in the cells while a better
537 health keeps the population size small. In addition, yeast cells with altruistic behaviour do not
538 give a boost to the population health as compared to selfish yeasts who although increase the
539 damage but doubles the size of the population. Providing good health to new buds
540 significantly increases damage in the mother cells which results in an early senescence state
541 where no more replications are possible (Aguilaniu et al., 2003; Denoth Lippuner et al., 2014;
542 Jazwinski and Wawryn, 2001; Liu et al., 2011; Spokoini et al., 2012). On the other hand, the
543 selfish behaviour allows a long replicative lifespan.

544 **Optimal Reproduction Success is Plausible to Local Minima of Cost Function**

545 Strategies were adopted for continuous search of the minimal value of the cost function. Since
546 the function values could not be anticipated in the stochastic simulations, the altruist value
547 varied continuously to search for it. Therefore, the cost function never converged to any
548 specific value. This interprets the physical phenomenon where mutations in a yeast strain
549 could vary the strategy that is followed by its progeny. It is observed that when yeast varied
550 its state from the minima of cost function, the subsequent mutations could not reverse
551 mutation due to stochastic effects and therefore the trait is able to reach local minima of the
552 cost function. Thus, the optimal reproduction success would never be able to show stable
553 behaviour near the minima of cost function. At the same time, when cells opted for minimum
554 value of cost function, the optimal reproduction success trapped for long period of time to
555 local minima which were surrounded by high cost functions.

556 **Evolutionary Ditches can make a Trait Maladaptive**

557 Evolutionary ditches became evolutionary traps in certain cases when the yeast species were
558 unable to escape from local minima because the cost function is surrounded by higher values.
559 With distance strategy, the cost function at $A = 1$ is lower than $0.5 < A < 1$, however it is
560 sufficiently higher than the minimum value of cost function (Figures 7 – 9). Consequently, in
561 the stochastic simulation, the cells with $A > 0.5$, have rapidly adapted complete altruist

behaviour, $A = 1$, and couldn't manage to escape from there. This behaviour showed sufficient potential in the yeast strategy to follow an extinction, especially when it is competing against the other species with lower values of cost function. In summary, our results suggest that damage retention during the early divisions (distance strategy) increases the number of healthy daughters in the yeast population. In addition, a rapid decrease in the efficiency of damage retention, at the time when the mother cell is almost exhausted, produces less daughters with very high amount of damage. Next, the two proposed strategies have distinct cost functions, implying that a strategy may not attain the same minima of cost function as the other. The minimum value attained by distance strategy has provided the minimal value of cost function. And finally, fluctuations in the cost function allow yeast cell to continuously vary its strategy, suggesting that optimal reproduction success is a local minimum of cost function.

Acknowledgment

This work was supported by the Swedish Foundation for Strategic Research.

577 Appendix 1

578 Mathematical model for yeast cell growth and division processes

579 In aging theory, replicative lifespan of a yeast cell is comprised of two major processes: cellular
580 growth in which the intact and damage components of a cell increase, and cell asymmetric
581 division in which cell buds out a new daughter cell. A pedigree-tree modelling approach is
582 used so that the cellular processes can be tracked for each cell individually. A similar modelling
583 approach has been used in the literature where the retention parameter was kept constant
584 (Erjavec et al., 2008), however it followed the fate of the progenitor and the progeny,
585 separately, through a number of generations. We could thus draw a “mother lineage” and a
586 “daughter lineage”, whereby we would, after every division, follow respectively the next
587 generation of mothers only, or the next generations of daughters only. However, these do not
588 represent a realistic population that consists of intermediated branches as well. Thus, in the
589 model presented here, we simulate the realistic population, including all intermediated
590 branches and mixed-linages.

591 During the growth process, the number of healthy protein (intact protein) molecules increases
592 in the cell at the rate constant k_1 and dissolves into the system due to half-life phenomenon
593 at the rate equals to k_2 . At the rate k_3 damage proteins are formed. The degradation rate for
594 damaged molecules is denoted by k_4 . The modelled equations can therefore be written as,

$$\begin{aligned} \dot{I} &= k_1 \left(1 - \frac{I + D}{K} \right) - k_2 I - k_3 I \\ \dot{D} &= k_3 I - k_4 D \end{aligned} \quad \text{Eq. 1}$$

595 The increase in the number of damaged proteins D becomes lethal if the cell reaches death
596 threshold value $D = D^*$ whereas the intact component I increases inside the cell to division
597 threshold $I = I^*$. If the cell reaches division threshold first, the cell divides and produces a
598 daughter cell with a mother to daughter cell size ratio $R_m : 1 - R_m$. During the early cell
599 divisions, the mother cell retains maximum damage while its retention efficiency decreases in
600 the later divisions until it reaches the minimum value $re(g)=0$, i.e. no retention.

601

Parameter	Description	Values	Assumptions and source
I^*	cell division threshold, in number of intact proteins	1500	amount of intact proteins (Erjavec et al., 2008)
D^*	cell death threshold, in number of damaged proteins	600	
k_1	rate maximal protein production	1.5×10^4	adjusted by hand to allow steady-state (Erjavec et al., 2008)
k_2	rate of degradation of intact proteins	$\ln 2$	half-life of 1 time unit (Erjavec et al., 2008)
k_3	rate of damaging of intact proteins	[0.1,2.3] by 0.75	(Erjavec et al., 2008)
k_4	rate of degradation of damaged proteins	$\ln 2$	half-life of 1 time unit (Erjavec et al., 2008)
K	carrying capacity	2500	adjusted by hand
re	retention coefficient	[0, 1] by 0.125	(Erjavec et al., 2008)
R_m	size of the progenitor after division	0.79	$R_m + R_d = 1$ (Erjavec et al., 2008)
R_d	size of the progeny after division	0.21	$R_m + R_d = 1$ (Erjavec et al., 2008)

Table 1: **Model parameters with default values and assumptions made**

605 The division process is modelled as discrete set of equations for mother and daughter cells.

606 For the mother cell, the intact and damage portions can be calculated as:

$$\begin{aligned} I_{in}(g+1) &= I_{end}(g) \cdot R_m - D_{end}(g) \cdot R_d \cdot re(g) \\ D_{in}(g+1) &= D_{end}(g) \cdot R_m + D_{end}(g) \cdot R_d \cdot re(g) \end{aligned} \quad \text{Eq. 2}$$

607 The intact and damage portions for daughter cells have the similar equations

$$\begin{aligned} I_{in}(g+1) &= I_{end}(g) \cdot R_d + D_{end}(g) \cdot R_d \cdot re(g) \\ D_{in}(g+1) &= D_{end}(g) \cdot R_d - D_{end}(g) \cdot R_d \cdot re(g) \end{aligned} \quad \text{Eq. 3}$$

608 where the parameter $R_d = 1 - R_m$ size of the daughter cell after division and g is division
609 number. The index terms *in* and *end* are the initial value after division and end value before
610 division respectively. The equations 2 and 3 are based on the principle of mass conservation
611 over generations (Erjavec et al., 2008). In particular, this means that the total cellular content
612 ($I+D$), in the original cell equal the sum of the total cellular content of the mother and daughter
613 cell. The conditions are also based on mass conservation with respect to intact component I
614 and damage D .

615 General behaviour of Model

616 The processes described in the above model involving cellular growth and division processes
617 are simulated in the *Figure S1*. The figure describes a general behaviour of the modelled system
618 without including the strategies and their altruist behaviour. Three parameters are
619 investigated at different values to understand their effect on the overall dynamics of the
620 modelled system. We observe that cell undergoes more number of divisions with the decrease
621 in the values of k_3 , R_m and re . In case of finite replications, cell generally takes more time in
622 the later divisions to grow and reach the division threshold. On the other hand, increasing the
623 cell size ratio from mother to daughter cells (R_m) decreases the time to next division. Damage
624 retention also plays an important role in replicative lifespan of a cell. However, this parameter
625 is chosen constant here for the sake of simplicity. It is interesting to observe that total number
626 of divisions drastically decreases with the increase in retention parameter. We study the
627 retention parameter as variable, dependent upon number of divisions of the mother cell.

628

629

630

631

632

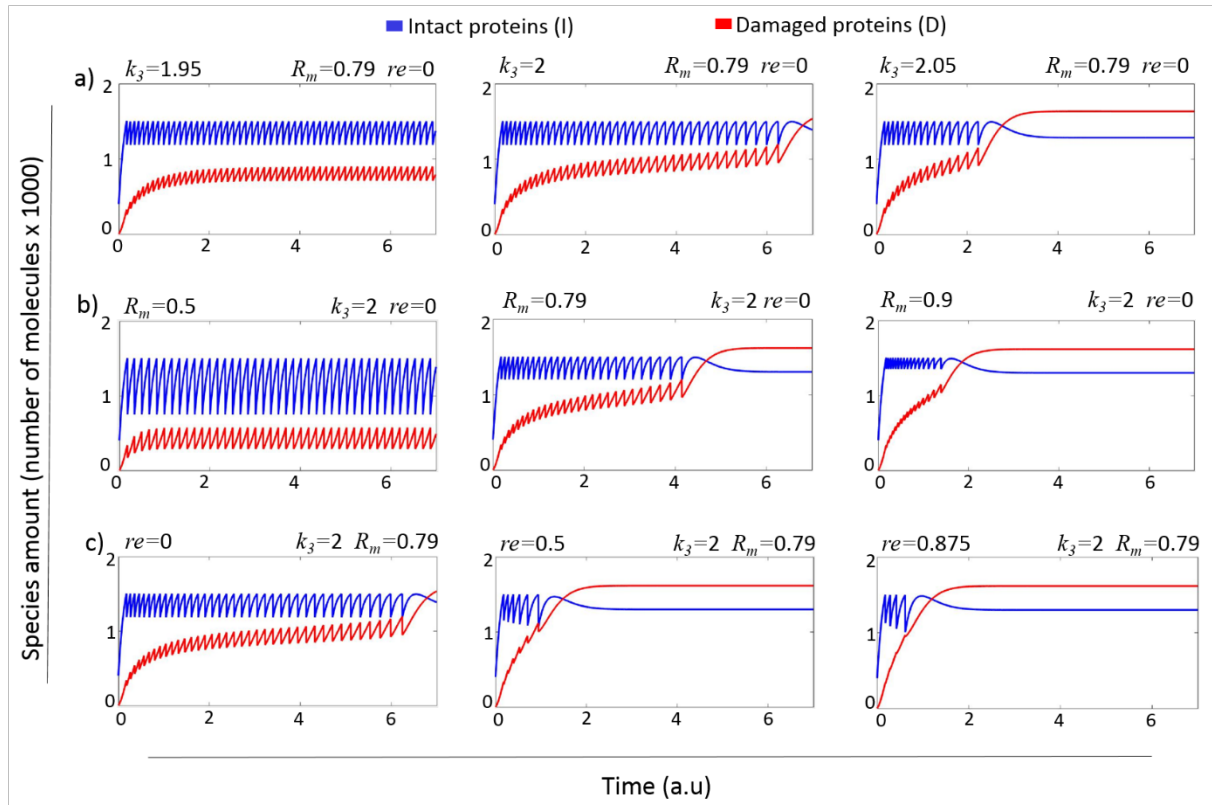


Figure S1: Intracellular species dynamics of a single cell a) damage accumulation rates b) size of the mother and c) retention coefficients. Red and blue lines describe the dynamics of damaged and intact cellular components, respectively. $re(g) = Re$ (a constant).

Pedigree-Tree Diagram

Pedigree-tree model follows growth and division process of each individual cell. The process starts with a single cell that grows its intact and damaged component. At the growth threshold, cell buds its first daughter cell. At this time point, the budding cell is considered as mother while the budded cell is considered as daughter cell. Now mother cell and daughter cell both undergoes the growth process to reach the division threshold, see Figure S2. Hence cell population increases while each cell is tracked during its replicative lifespan or until the simulation ends. Population is discretely distributed over the total intact and damage portions of each cell as described in the main text.

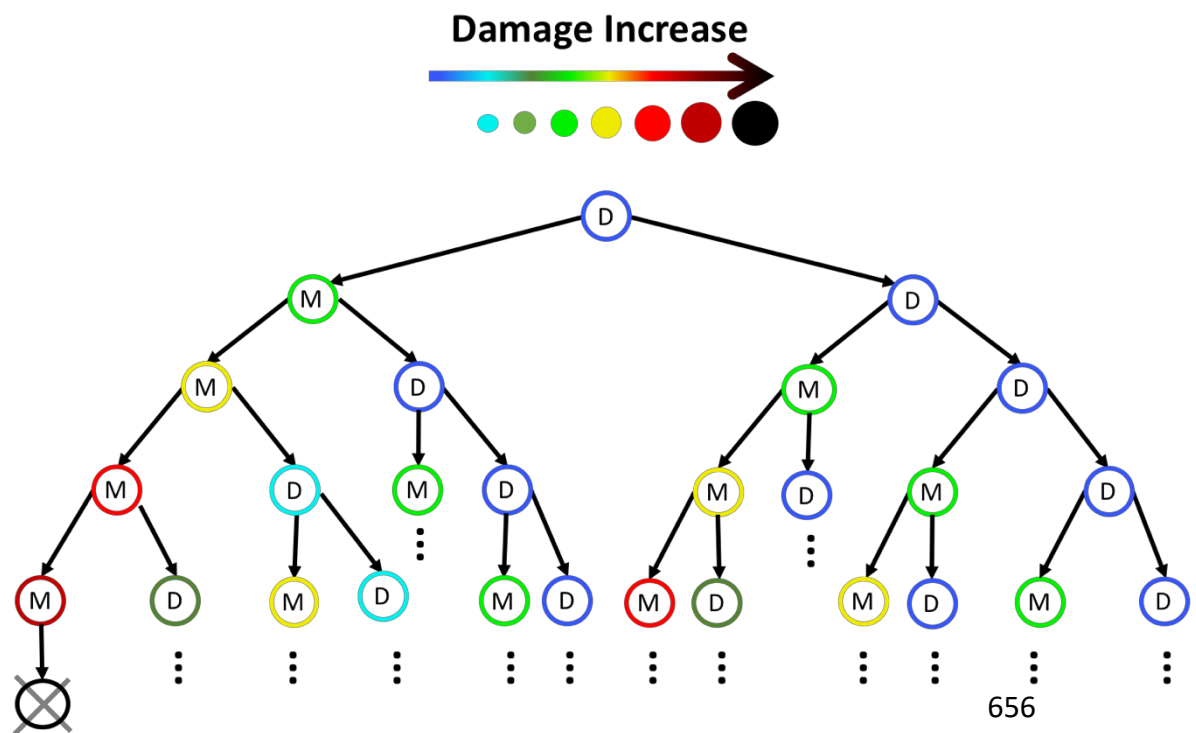


Figure S2: Schematic representation of pedigree-tree model. Each circle represents a cell. D stands for daughter whereas M stands for mother. Blue color is damage free cells while black color is for dead cells (no more divisions possible).

Appendix 2

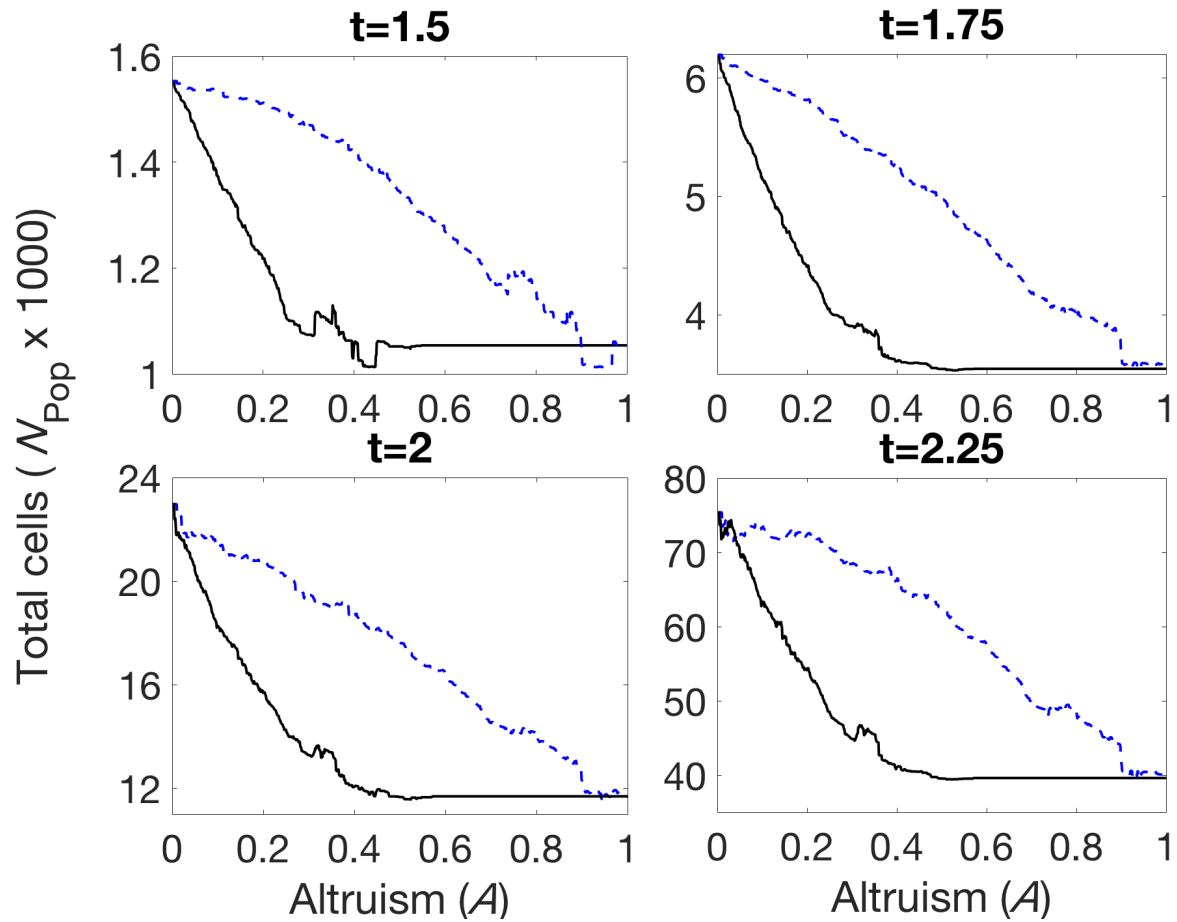


Figure S3: Total number of cells against the altruism values at four simulation times $t = 1.5, 1.75, 2, 2.25$. Lines represents population with distance strategy whereas the dashed lines represent the population with division strategy.

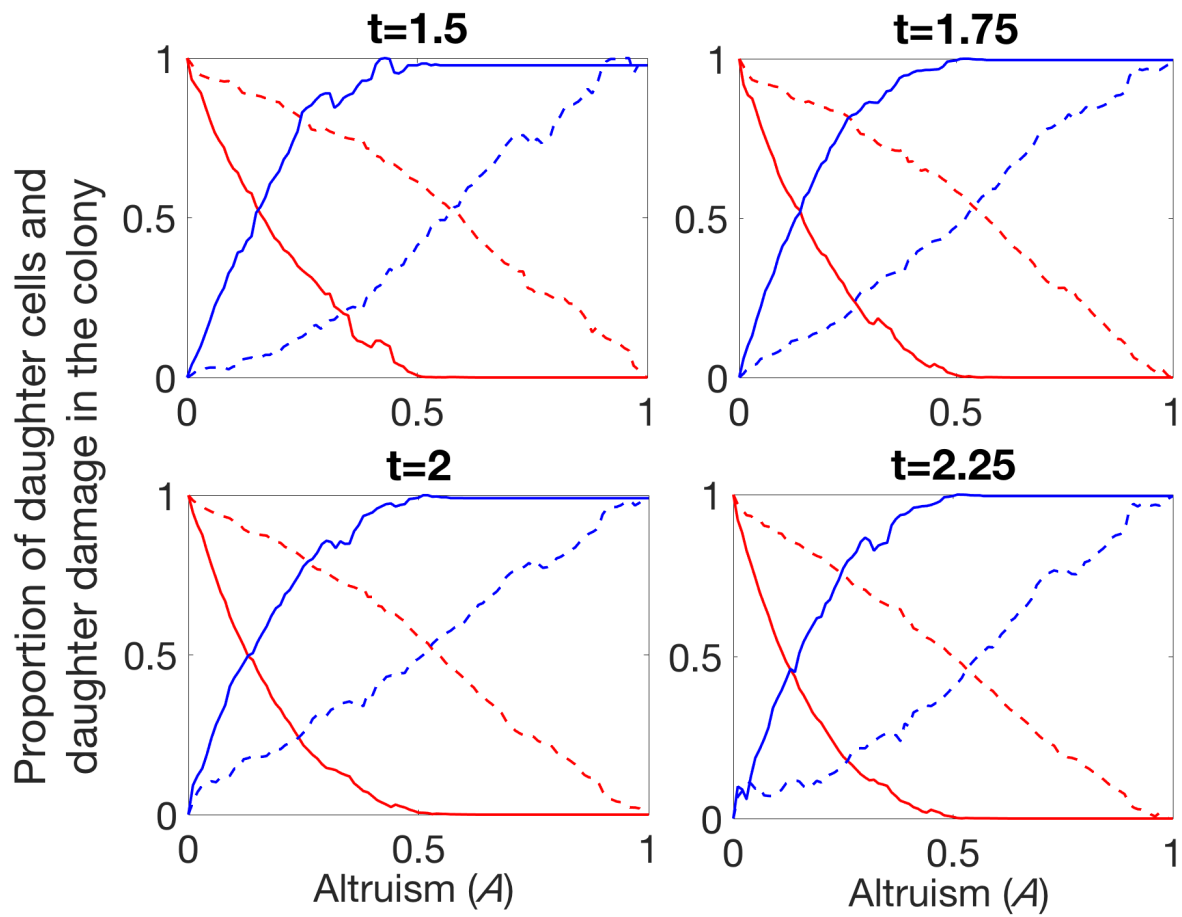


Figure S4: Proportion of daughter cells and their damage in the population for time $t = 1.5, 1.75, 2$ and 2.25 . The continuous lines represent distance strategy while dashed lines represent division strategy. The lines moving from 0 to 1 are the daughter cells proportion while the lines moving from 1 to 0 are the damage proportion.

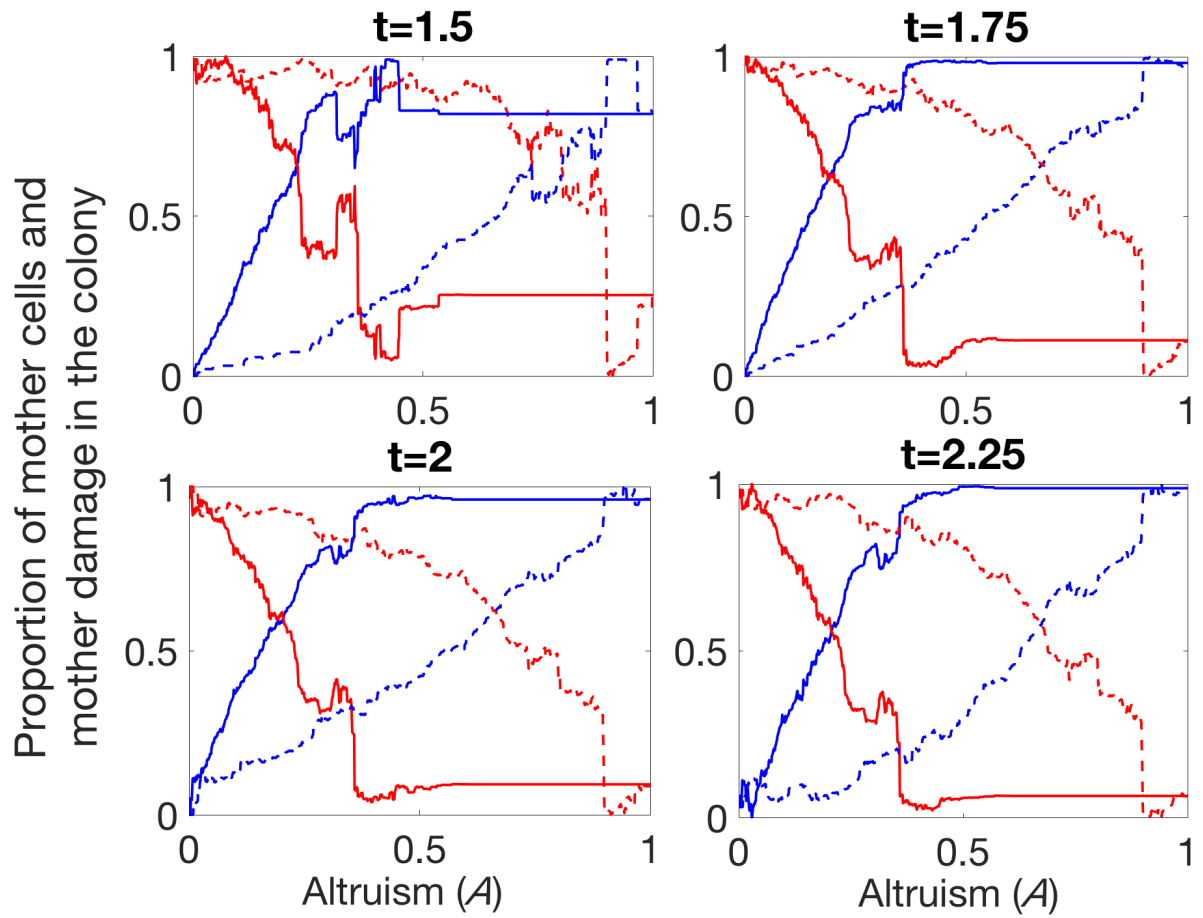


Figure S5: Proportion of mother cells and their damage in the colony at time $t = 1.5, 1.75, 2$ and 2.25 . The continuous lines represent distance strategy while dashed lines represent division strategy. The lines moving from 0 to 1 along y-axis are the mother cells proportion while the lines moving from 1 to 0 are the damage proportion.

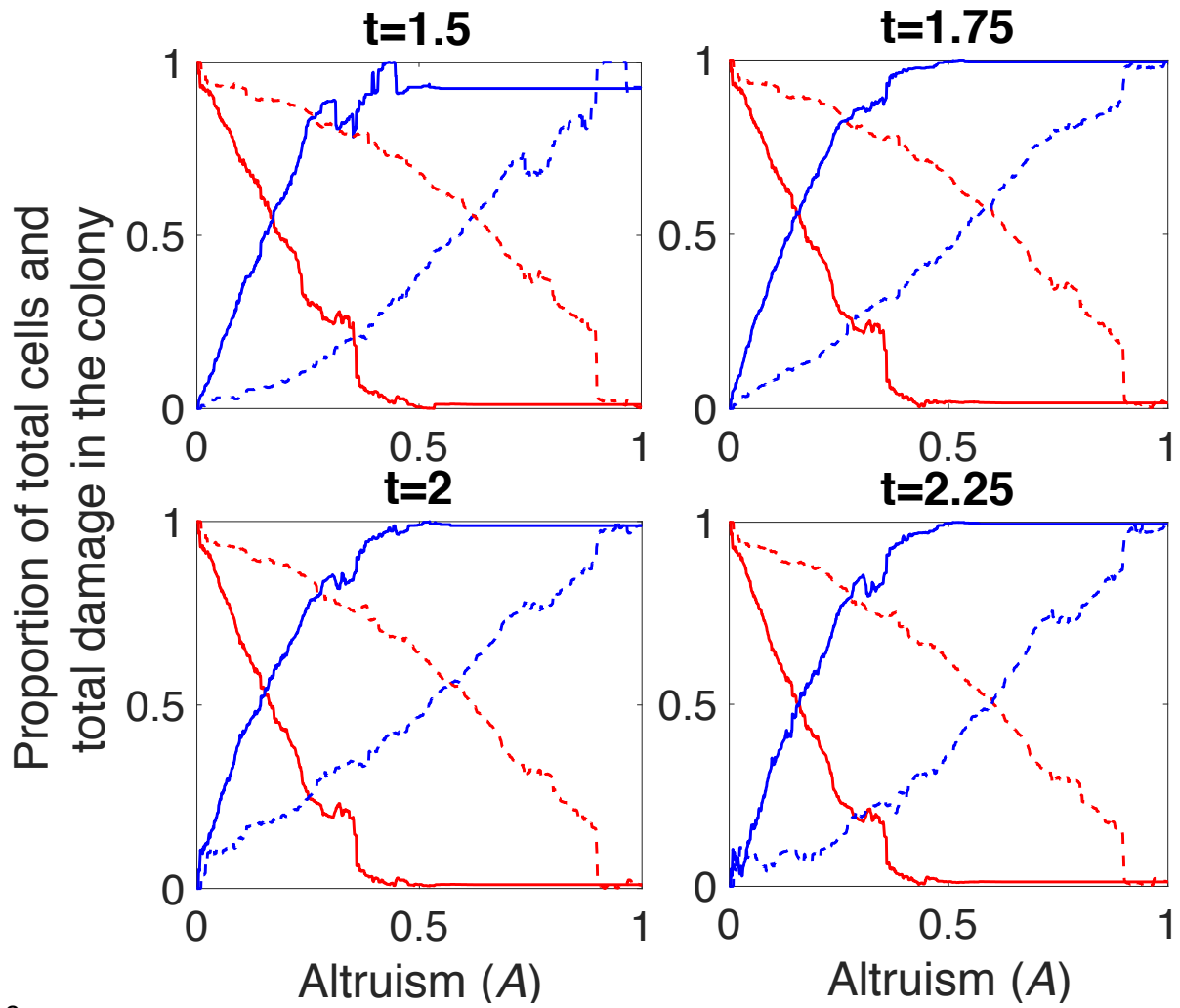


Figure S6: Proportion of total cells and their damage in the population for time $t = 1.5, 1.75, 2$ and 2.25 . The continuous lines represent distance strategy while dashed lines represent division strategy. The lines moving from 0 to 1 are the total cells proportion while the lines moving from 1 to 0 are the damage proportion.

721 **References**

- 722 Ackermann, M., Chao, L., Bergstrom, C.T., Doebeli, M., 2007. On the evolutionary origin of
723 aging. *Aging Cell* 6, 235–244. <https://doi.org/10.1111/j.1474-9726.2007.00281.x>
- 724 Ackermann, M., Stearns, S.C., Jenal, U., 2003. Senescence in a bacterium with asymmetric
725 division. *Science* 300, 1920. <https://doi.org/10.1126/science.1083532>
- 726 Aguilaniu, H., Gustafsson, L., Rigoulet, M., Nyström, T., 2003. Asymmetric inheritance of
727 oxidatively damaged proteins during cytokinesis. *Science* 299, 1751–1753.
728 <https://doi.org/10.1126/science.1080418>
- 729 Berg, J.M., Tymoczko, J.L., Stryer, L., 2002. *Evolution Requires Reproduction, Variation, and*
730 *Selective Pressure.*
- 731 Biesalski, H.K., 2002. Free radical theory of aging. *Curr. Opin. Clin. Nutr. Metab. Care* 5, 5–10.
- 732 Brooks, R.C., Garratt, M.G., 2017. Life history evolution, reproduction, and the origins of sex-
733 dependent aging and longevity. *Ann. N. Y. Acad. Sci.* 1389, 92–107.
734 <https://doi.org/10.1111/nyas.13302>
- 735 Bufalino, M.R., DeVeale, B., van der Kooy, D., 2013. The asymmetric segregation of damaged
736 proteins is stem cell-type dependent. *J. Cell Biol.* 201, 523–530.
737 <https://doi.org/10.1083/jcb.201207052>
- 738 Chao, L., 2010. A model for damage load and its implications for the evolution of bacterial
739 aging. *PLoS Genet.* 6. <https://doi.org/10.1371/journal.pgen.1001076>
- 740 Chao, L., Rang, C.U., Proenca, A.M., Chao, J.U., 2016. Asymmetrical Damage Partitioning in
741 Bacteria: A Model for the Evolution of Stochasticity, Determinism, and Genetic
742 Assimilation. *PLoS Comput. Biol.* 12. <https://doi.org/10.1371/journal.pcbi.1004700>
- 743 Clegg, R.J., Dyson, R.J., Kreft, J.-U., 2014. Repair rather than segregation of damage is the
744 optimal unicellular aging strategy. *BMC Biol.* 12. [https://doi.org/10.1186/s12915-014-](https://doi.org/10.1186/s12915-014-0052-x)
745 0052-x
- 746 Coelho, M., Lade, S.J., Alberti, S., Gross, T., Tolić, I.M., 2014. Fusion of protein aggregates
747 facilitates asymmetric damage segregation. *PLoS Biol.* 12, e1001886.
748 <https://doi.org/10.1371/journal.pbio.1001886>
- 749 de Grey, A.D., 1997. A proposed refinement of the mitochondrial free radical theory of aging.
750 *BioEssays News Rev. Mol. Cell. Dev. Biol.* 19, 161–166.
751 <https://doi.org/10.1002/bies.950190211>
- 752 Denoth Lippuner, A., Julou, T., Barral, Y., 2014. Budding yeast as a model organism to study
753 the effects of age. *FEMS Microbiol. Rev.* 38, 300–325. [https://doi.org/10.1111/1574-](https://doi.org/10.1111/1574-6976.12060)
754 6976.12060

755 Egilmez, N. K, and Jazwinski, S.M., 1989. Evidence for the involvement of a cytoplasmic factor
756 in the aging of the yeast *Saccharomyces cerevisiae*. *J Bacteriol* 171: 37–42.

757 Erjavec, N., Cvijovic, M., Klipp, E., Nyström, T., 2008. Selective benefits of damage partitioning
758 in unicellular systems and its effects on aging. *Proc. Natl. Acad. Sci. U. S. A.* 105, 18764–
759 18769. <https://doi.org/10.1073/pnas.0804550105>

760 Erjavec, N., Larsson, L., Grantham, J., Nyström, T., 2007. Accelerated aging and failure to
761 segregate damaged proteins in Sir2 mutants can be suppressed by overproducing the
762 protein aggregation-remodeling factor Hsp104p. *Genes Dev.* 21, 2410–2421.
763 <https://doi.org/10.1101/gad.439307>

764 Hill, S.M., Hanzén, S., Nyström, T., 2017. Restricted access: spatial sequestration of damaged
765 proteins during stress and aging. *EMBO Rep.* 18, 377–391.
766 <https://doi.org/10.15252/embr.201643458>

767 Hill, S.M., Hao, X., Grönvall, J., Spikings-Nordby, S., Widlund, P.O., Amen, T., Jörhov, A.,
768 Josefson, R., Kaganovich, D., Liu, B., Nyström, T., 2016. Asymmetric Inheritance of
769 Aggregated Proteins and Age Reset in Yeast Are Regulated by Vac17-Dependent
770 Vacuolar Functions. *Cell Rep.* 16, 826–838.
771 <https://doi.org/10.1016/j.celrep.2016.06.016>

772 Jazwinski, S.M., Wawryn, J., 2001. Profiles of random change during aging contain hidden
773 information about longevity and the aging process. *J. Theor. Biol.* 213, 599–608.
774 <https://doi.org/10.1006/jtbi.2001.2434>

775 Kaeberlein, M., 2010. Lessons on longevity from budding yeast. *Nature* 464: 513–519.

776 Katajisto, P., Döhla, J., Chaffer, C., Pentinmikko, N., Marjanovic, N., Iqbal, S., Zoncu, R., Chen,
777 W., Weinberg, R.A., Sabatini, D.M., 2015. Asymmetric apportioning of aged
778 mitochondria between daughter cells is required for stemness. *Science* 348, 340–343.
779 <https://doi.org/10.1126/science.1260384>

780 Kennedy, B.K., Austriaco, N.R., Guarente, L., 1994. Daughter cells of *Saccharomyces cerevisiae*
781 from old mothers display a reduced life span. *J. Cell Biol.* 127, 1985–1993.

782 Kirkwood, T.B., Rose, M.R., 1991. Evolution of senescence: late survival sacrificed for
783 reproduction. *Philos. Trans. R. Soc. Lond. B. Biol. Sci.* 332, 15–24.
784 <https://doi.org/10.1098/rstb.1991.0028>

785 Konieczny, L., Roterman-Konieczna, I., Spólnik, P., 2014. The Structure and Function of Living
786 Organisms, in: *Systems Biology*. Springer, Cham, pp. 1–32.
787 https://doi.org/10.1007/978-3-319-01336-7_1

788 Kowald, A., Kirkwood, T.B., 2000. Accumulation of defective mitochondria through delayed
789 degradation of damaged organelles and its possible role in the ageing of post-mitotic
790 and dividing cells. *J. Theor. Biol.* 202, 145–160. <https://doi.org/10.1006/jtbi.1999.1046>

791 Kruegel, U., Robison, B., Dange, T., Kahlert, G., Delaney, J.R., Kotireddy, S., Tsuchiya, M.,
792 Tsuchiyama, S., Murakami, C.J., Schleit, J., Sutphin, G., Carr, D., Tar, K., Dittmar, G.,
793 Kaeberlein, M., Kennedy, B.K., Schmidt, M., 2011. Elevated proteasome capacity
794 extends replicative lifespan in *Saccharomyces cerevisiae*. *PLoS Genet.* 7, e1002253.
795 <https://doi.org/10.1371/journal.pgen.1002253>

796 Lindner, A.B., Madden, R., Demarez, A., Stewart, E.J., Taddei, F., 2008. Asymmetric segregation
797 of protein aggregates is associated with cellular aging and rejuvenation. *Proc. Natl.*
798 *Acad. Sci. U. S. A.* 105, 3076–3081. <https://doi.org/10.1073/pnas.0708931105>

799 Liu, B., Larsson, L., Franssens, V., Hao, X., Hill, S.M., Andersson, V., Höglund, D., Song, J., Yang,
800 X., Öling, D., Grantham, J., Winderickx, J., Nyström, T., 2011. Segregation of protein
801 aggregates involves actin and the polarity machinery. *Cell* 147, 959–961.
802 <https://doi.org/10.1016/j.cell.2011.11.018>

803 Longo, V., Shadel, G. S., Kaeberlein, M., Kennedy, B., 2012. Replicative and Chronological Ageing
804 in *Saccharomyces cerevisiae* *Cell Metab.* 16(1): 18-31 <https://doi.org/10.1016/j.cmet.2012.06.002>

806 Nyström, T., Liu, B., 2014. Protein quality control in time and space - links to cellular aging.
807 *FEMS Yeast Res.* 14, 40–48. <https://doi.org/10.1111/1567-1364.12095>

808 Orgel, L.E., 1963. The maintenance of the accuracy of protein synthesis and its relevance to
809 ageing. *Proc. Natl. Acad. Sci. U. S. A.* 49, 517–521.

810 Rujano, M.A., Bosveld, F., Salomons, F.A., Dijk, F., van Waarde, M.A.W.H., van der Want, J.J.L.,
811 de Vos, R.A.I., Brunt, E.R., Sibon, O.C.M., Kampinga, H.H., 2006. Polarised asymmetric
812 inheritance of accumulated protein damage in higher eukaryotes. *PLoS Biol.* 4, e417.
813 <https://doi.org/10.1371/journal.pbio.0040417>

814 Spokoini, R., Moldavski, O., Nahmias, Y., England, J.L., Schuldiner, M., Kaganovich, D., 2012.
815 Confinement to organelle-associated inclusion structures mediates asymmetric
816 inheritance of aggregated protein in budding yeast. *Cell Rep.* 2, 738–747.
817 <https://doi.org/10.1016/j.celrep.2012.08.024>

818 Stewart, E.J., Madden, R., Paul, G., Taddei, F., 2005. Aging and Death in an Organism That
819 Reproduces by Morphologically Symmetric Division. *PLoS Biol.* 3.
820 <https://doi.org/10.1371/journal.pbio.0030045>

821 Tyedmers, J., Mogk, A., Bukau, B., 2010. Cellular strategies for controlling protein aggregation.
822 *Nat. Rev. Mol. Cell Biol.* 11, 777–788. <https://doi.org/10.1038/nrm2993>

823 Vedel, S., Nunns, H., Košmrlj, A., Semsey, S., Trusina, A., 2016. Asymmetric Damage
824 Segregation Constitutes an Emergent Population-Level Stress Response. *Cell Syst.* 3,
825 187–198. <https://doi.org/10.1016/j.cels.2016.06.008>

826 Zhou, C., Slaughter, B.D., Unruh, J.R., Guo, F., Yu, Z., Mickey, K., Narkar, A., Ross, R.T., McClain,
827 M., Li, R., 2014. Organelle-based aggregation and retention of damaged proteins in

828 asymmetrically dividing cells. Cell 159, 530–542.
829 <https://doi.org/10.1016/j.cell.2014.09.026>

830